



## Article

# C2CD4B Evokes Oxidative Stress and Vascular Dysfunction via a PI3K/Akt/PKC $\alpha$ -Signaling Pathway

Paola Di Pietro <sup>1</sup>, Angela Carmelita Abate <sup>1</sup>, Valeria Prete <sup>1</sup>, Antonio Damato <sup>2</sup>, Eleonora Venturini <sup>2</sup>, Maria Rosaria Rusciano <sup>1</sup>, Carmine Izzo <sup>1</sup>, Valeria Visco <sup>1</sup>, Michele Ciccarelli <sup>1</sup>, Carmine Vecchione <sup>1,2</sup> and Albino Carrizzo <sup>1,2,\*</sup>

<sup>1</sup> Department of Medicine, Surgery and Dentistry “Scuola Medica Salernitana”, University of Salerno, 84081 Baronissi, Italy; pdipietro@unisa.it (P.D.P.); aabate@unisa.it (A.C.A.); valeria.prete97@gmail.com (V.P.); mrusciano@unisa.it (M.R.R.); carmine.izzo93@gmail.com (C.I.); vvisco@unisa.it (V.V.); mciccarelli@unisa.it (M.C.); cvecchione@unisa.it (C.V.)

<sup>2</sup> Vascular Physiopathology Unit, IRCCS Neuromed, 86077 Pozzilli, Italy; antonio.damato85@gmail.com (A.D.); eleonora.venturini94@libero.it (E.V.)

\* Correspondence: acarizzo@unisa.it

**Abstract:** High glucose-induced endothelial dysfunction is an important pathological feature of diabetic vasculopathy. While genome-wide studies have identified an association between type 2 diabetes mellitus (T2DM) and increased expression of a C2 calcium-dependent domain containing 4B (C2CD4B), no study has yet explored the possible direct effect of C2CD4B on vascular function. Vascular reactivity studies were conducted using a pressure myograph, and nitric oxide and oxidative stress were assessed through difluorofluorescein diacetate and dihydroethidium, respectively. We demonstrate that high glucose upregulated both mRNA and protein expression of C2CD4B in mice mesenteric arteries in a time-dependent manner. Notably, the inhibition of C2CD4B expression by genetic knockdown efficiently prevented hyperglycemia-induced oxidative stress, endothelial dysfunction, and loss of nitric oxide (NO) bioavailability. Recombinant C2CD4B evoked endothelial dysfunction of mice mesenteric arteries, an effect associated with increased reactive oxygen species (ROS) and decreased NO production. In isolated human umbilical vein endothelial cells (HUVECs), C2CD4B increased phosphorylation of endothelial nitric oxide synthase (eNOS) at the inhibitory site Thr495 and reduced eNOS dimerization. Pharmacological inhibitors of phosphoinositide 3-kinase (PI3K), Akt, and PKC $\alpha$  effectively attenuated oxidative stress, NO reduction, impairment of endothelial function, and eNOS uncoupling induced by C2CD4B. These data demonstrate, for the first time, that C2CD4B exerts a direct effect on vascular endothelium via a phosphoinositide 3-kinase (PI3K)/Akt/PKC $\alpha$ -signaling pathway, providing a new perspective on C2CD4B as a promising therapeutic target for the prevention of oxidative stress in diabetes-induced endothelial dysfunction.

**Keywords:** C2CD4B; endothelial dysfunction; oxidative stress; eNOS uncoupling; diabetes



**Citation:** Di Pietro, P.; Abate, A.C.; Prete, V.; Damato, A.; Venturini, E.; Rusciano, M.R.; Izzo, C.; Visco, V.; Ciccarelli, M.; Vecchione, C.; et al. C2CD4B Evokes Oxidative Stress and Vascular Dysfunction via a PI3K/Akt/PKC $\alpha$ -Signaling Pathway. *Antioxidants* **2024**, *13*, 101. <https://doi.org/10.3390/antiox13010101>

Academic Editor: Alessandra Napolitano

Received: 29 November 2023

Revised: 11 January 2024

Accepted: 12 January 2024

Published: 14 January 2024



**Copyright:** © 2024 by the authors. Licensee MDPI, Basel, Switzerland. This article is an open access article distributed under the terms and conditions of the Creative Commons Attribution (CC BY) license (<https://creativecommons.org/licenses/by/4.0/>).

## 1. Introduction

More than 450 million people worldwide are estimated to be living with diabetes mellitus, a prevalence anticipated to increase by 25% in 2030 and 51% in 2045 [1,2]. The rise in morbidity and mortality among diabetic patients is primarily attributed to the onset of cardiovascular disease (CVD) [3], where vascular complications represent the most severe clinical manifestations of the disease.

Chronic hyperglycemia has been shown to activate oxidative stress-generating machinery, leading to vascular dysfunction in mice [4,5]. Among the vascular cells, endothelial cell (EC) dysfunction emerges as the primary mediator of vascular complications [6]. In diabetic patients, endothelial dysfunction is acknowledged as a critical contributor to vascular disease pathogenesis, often preceding diabetes development [7–10].

Despite these insights, there are few therapies specifically targeting oxidative stress and vascular disease alterations in diabetes. Identifying previously unknown molecules involved in hyperglycemia-induced endothelial damage could pave the way for new therapeutic approaches to prevent or slow down the progression of diabetes-associated vascular complications.

C2CD4B is a protein predominantly found in pancreatic and endothelial cells, where it plays a role in beta cell differentiation [11], and in the regulation of cell architecture and adhesion [12].

Previous studies have suggested that C2CD4B may regulate vascular permeability and factors implicated in thrombotic events [12,13]. A genome-wide significant association was found between the VPS13C/C2CD4A/C2CD4B locus and T2DM risk [14–18]. Subsequent studies revealed that single nucleotide polymorphisms (SNPs) located in close proximity to the C2CD4B gene were associated with diabetes-related traits [19,20], including increased fasting plasma glucose [21], proinsulin levels [22] and impaired beta cell function [23].

The present study aims to shed light on the potential effects of C2CD4B on EC and vascular function in mice resistance arteries. Using mice mesenteric arteries, we demonstrate for the first time that recombinant C2CD4B promotes excessive ROS production and impairs nitric oxide signaling, leading to vascular dysfunction through a PI3K/Akt/PKC $\alpha$ -dependent pathway. We show that C2CD4B is required for the development of endothelial dysfunction in hyperglycemic conditions. In terms of its therapeutic implication mechanism, we demonstrate that gene silencing of C2CD4B protects against oxidative stress and endothelial dysfunction induced by hyperglycemic conditions. Thus, targeting C2CD4B opens a new therapeutic avenue for preventing vascular complications in patients with diabetes mellitus.

## 2. Materials and Methods

### 2.1. Reagents

To characterize molecular signaling, mesenteric arteries or HUVECs were pre-treated, or not, before data were obtained with the following: tempol (100  $\mu$ M for 1 h; Cat. 176141; Sigma-Aldrich, Merck Life Science S.r.l., Milano, Italy); the NOS inhibitor N- $\omega$ -nitro-L-arginine methyl ester (L-NAME, 300  $\mu$ mol/L for 30 min, Sigma-Aldrich, Cat. N5751); the phosphatidylinositol-4,5-bisphosphate 3-kinase inhibitor (wortmannin; Cat. 1232; Tocris Bioscience, Space Import-Export, Milano, Italy); the AKT inhibitor X (Sigma-Aldrich, Cat. 124020); Go6976 (Tocris Bioscience, Cat. 2253). Recombinant human C2CD4B protein (Cat. MBS1165211) was purchased from MyBioSource (S.I.A.L. s.r.l., Rome, Italy).

### 2.2. Cell Culture and Treatment

Human umbilical vein endothelial cells (HUVEC; CRL-4053) were purchased from American Type Culture Collection (ATCC) and cultured in Vascular Cell Basal Medium (ATCC PCS-100-030) supplemented with Endothelial Cell Growth Kit (ATCC PCS-110-041), penicillin (100 U/mL), and streptomycin (100 U/mL). Cells were maintained at 37 °C and 5% CO<sub>2</sub> in a humidified incubator. To evaluate effects of C2CD4B, cells were cultured for 1 h with the recombinant protein (100 ng/mL). To characterize intracellular signaling, HUVECs were pretreated with the following pharmacological inhibitors: phosphatidylinositol-4,5-bisphosphate 3-kinase inhibitor (wortmannin, 10  $\mu$ M, 1 h); the AKT inhibitor X (10  $\mu$ M, 1 h); and Go6976 (500 nM, 30 min).

### 2.3. Mice

All animal experiments were carried out in accordance with the Guide for the Care and Use of Laboratory Animals published by the US National Institutes of Health and approved by the Ethical Committee of Istituto Neurologico Mediterraneo IRCCS Neuromed (Ethical protocol code: 570/2019PR). Mice were maintained in a 22 °C room with a 12 h light/dark cycle, and received food and water ad libitum. Vascular reactivity and molecular

studies were performed on 8–10 weeks-old wild-type male C57BL/6 mice (weighing 25–30 g) (Jackson Laboratories, Bar Harbor, ME, USA).

#### 2.4. Determination of mRNA Expression Level of C2CD4B

RNA was extracted with TRI reagent (Sigma-Aldrich), quantified by NanoDrop 1000 spectrophotometer (Thermo Fisher Scientific, Milan, Italy), treated with DNase I (Invitrogen, Milan, Italy), and reverse transcribed using a SuperScript VILO Master Mix (Invitrogen, Cat. 11755500). Specific cDNAs were amplified and analyzed using a 7500 Real-Time PCR System (Applied Biosciences, Milan, Italy). Quantification of the relative expression levels was performed using  $\Delta$ CT calculation. The sequences of primers used for qRT-PCR are the following: C2CD4B, FW: 5'-GACCGCGAAGACAGTGACGAAG-3'; RV: 5'-CGCAGAAGCCGTAAACGGTGC-3'; GAPDH, FW: 5'-CGTCCCGTAGACAAAATGGT-3'; RV: 5'-TCAATGAAGGGGTCGTTGAT-3'.

#### 2.5. Vascular Reactivity Studies

Vascular reactivity studies were performed as previously described [24]. In brief, mice mesenteric arteries were mounted in a wire or pressure myograph system containing Krebs solution (pH 7.4 at 37 °C in oxygenated 95% O<sub>2</sub>/5% CO<sub>2</sub>). An amount of 80 mmol/L of KCl was used to evaluate the vasoconstrictive response at the basal level. Phenylephrine (10<sup>-9</sup> M to 10<sup>-6</sup> M) was used to reproduce 80% of maximal contraction. Acetylcholine (10<sup>-9</sup> M to 10<sup>-6</sup> M) was used to evaluate endothelial-dependent vasodilator response. Mesenteric arteries were treated with recombinant C2CD4B (100 µg/mL) for 1 h.

#### 2.6. Gene Silencing

Second-order branches of the mesenteric arterial tree were removed from C57BL/6 mice and transfected with siRNA against *C2cd4b* (sc-108918; Santa Cruz Biotechnology Inc.; S.I.A.L. s.r.l., Rome, Italy) and its relative scramble sequence as previously described [25]. Vessels were placed in a Mulvany pressure system filled with Krebs solution and 100 nM of siRNA vector. All vessels were perfused at 100 mmHg for 1 h and then at 60 mmHg for 5 h. Endothelium-dependent and -independent relaxation was assessed by measuring the dilatory responses of mesenteric arteries to cumulative concentrations of acetylcholine (from 10<sup>-9</sup> M to 10<sup>-5</sup> M), in vessels precontracted with U46619 at a dose necessary to obtain a similar level of precontraction (80% of initial KCl-evoked contraction) in each vessel. Values are reported as a percentage of lumen diameter change after exposure to the substance.

#### 2.7. Evaluation of ROS Production

To determine eNOS-dependent ROS formation, mesenteric arteries were preincubated with the NOS inhibitor L-NAME (300 µM for 30 min), embedded in Tissue Tek resin, frozen and cryo-sectioned (7 µm) using a cryostat (Leica CM1950, Leica Microsystems, Wetzlar, Germany). In detail, ROS production was evaluated by dihydroethidium staining (DHE, Life Technologies, Carlsbad, CA, USA), as previously described [26]. Briefly, sections were washed in PBS at 37 °C for 10 min and then incubated with DHE (5 µM, Sigma-Aldrich, Cat. D7008) in a humidified chamber protected from light at 37 °C for 30 min. Slices were washed with PBS 1X, and then mounted on a glass slide. Images were observed and acquired under a Nikon Eclipse Ti-E fluorescence microscope (Nikon, Milan, Italy). Fluorescence intensity was measured using ImageJ software.

ROS production in HUVECs was quantified with the membrane-permeable fluorescent probe, Dihydrorhodamine 123 (DHR123) (Thermo Fisher Scientific, Cat. D23806). HUVECs seeded on a microplate were washed with PBS 1X and then treated with DHR123 (10 µM) for 30 min. Fluorescence was determined using an Infinite Pro M200 Tecan microplate reader at a maximum excitation and emission spectra of 507 and 525 nm, respectively. NADPH-mediated superoxide radical production was determined using the lucigenin-enhanced chemiluminescence (ECL) assay, as previously described [25]. Briefly, after

reaching 80% confluence, HUVECs were washed with pre-warmed PBS 1X, detached using 0.25% trypsin/EDTA (1 mmol/L), and resuspended in modified HEPES buffer containing 140 mmol/L NaCl; 5 mmol/L KCl; 0.8 mmol/L MgCl<sub>2</sub>; 1.8 mmol/L CaCl<sub>2</sub>; 1 mmol/L Na<sub>2</sub>HPO<sub>4</sub>; 25 mmol/L HEPES; and 1% glucose, pH 7. Subsequently, cells were homogenized, and 100 µg of extract was distributed on a 96-well microplate. Protein content was determined by the Bradford method. The reaction was started by adding NADPH (0.1 mmol/L) and lucigenin (5 µmol/L) to each well. Chemiluminescence was measured using Tecan Infinite Pro M200 microplate reader at 37 °C.

### 2.8. Nitric Oxide Detection

NO production was evaluated using 4-amino-5-methylamino-2',7-difluorofluorescein diacetate (DAF-FM, Thermo Fisher Scientific, Cat. D23844). Mesenteric arteries were embedded in Tissue Tek resin, frozen, and cryo-sectioned at 7 µm. Sections were allowed to air-dry at room temperature, fixed with 2% paraformaldehyde for 20 min, and then washed with PBS. Subsequently, they were incubated with DAF-FM (20 µM) for 30 min at 37 °C in a light-protected humidified chamber, washed with PBS, and then mounted on a glass slide. Images were acquired using a fluorescence microscope (Nikon Eclipse Ti-E, Nikon Corp.), and DAF-FM-derived fluorescent intensity was determined using ImageJ software.

### 2.9. Immunoblotting

Protein extracts were separated on SDS-PAGE and then transferred onto a PVDF membrane. The membranes were incubated overnight with the following primary antibodies: anti-eNOS (Cat. #5880; Cell signaling Technology, Danvers, MA, USA); anti-phospho-PI3K (Abclonal, Rome, Italy, Cat. AP0854); anti-phospho-Akt (Cat. sc-7985; Santa Cruz Biotechnology, S.I.A.L. s.r.l., Rome, Italy); anti-β-actin (Cat. ab8226; Abcam, Prodotti Gianni, Milan, Italy); anti-phospho-PKCα (Abcam, Cat. ab76016), anti-α-tubulin (Cat. 627901; Biolegend, Campoverde S.r.l., Milan, Italy); anti-vinculin (Sigma-Aldrich, Cat. V4139); and anti-GAPDH (Santa Cruz Biotechnology, Cat. sc-32233). After a triple wash, membranes were incubated for 1 h with the HRP-conjugated secondary antibodies: anti-rabbit IgG (Invitrogen, Cat. 31463) or anti-mouse IgG (Cat. 31430; Invitrogen, Milan, Italy). Bands were visualized with ECL reagent (Thermo Fisher Scientific, Cat. 32209) according to the manufacturer's instructions. Immunoblotting data were analyzed using ImageJ software to determine optical density (OD) of the bands. The OD readings of phosphorylated proteins were expressed as a ratio relative to beta-actin or GAPDH.

### Detection of eNOS Dimer and Monomer

Non-reducing low-temperature SDS-PAGE (LT-PAGE) was performed to detect eNOS dimer and monomer. Briefly, the samples were incubated in O'Farrell's lysis buffer without (non-reducing) 2-mercaptoethanol at 37 °C for 5 min. Protein extracts were separated on 7.5% SDS-PAGE. Gel and buffers were equilibrated at 4 °C before electrophoresis, and the buffer tank was placed in an ice bath during electrophoresis to maintain the temperature of the gel < 15 °C. Subsequent to LT-PAGE, the gel was transferred, and the immunoblots were performed as previously described [27].

### 2.10. Statistical Analysis

Data are presented as mean ± SEM. Data sets were tested for normality of distribution with the Shapiro–Wilk or Kolmogorov–Smirnov test. Two-sided unpaired Student's *t*-test was used for comparisons between 2 independent groups. Data groups (comparisons across multiple groups) with normal distributions were compared using one-way ANOVA (with Bonferroni's correction), unless otherwise indicated. For comparison across different timepoints, data were analyzed using ordinary two-way ANOVA analysis followed by a Bonferroni multiple comparison test. Differences were considered to be statistically significant when  $p < 0.05$ .

### 3. Results

#### 3.1. Genetic Inhibition of C2CD4B Protects against High Glucose-Induced Oxidative Stress and Endothelial Dysfunction

C2CD4B belongs to the C2CD4 family, whose genes are encoded in a susceptibility locus for T2DM [14]. To investigate whether hyperglycemic conditions could modulate C2CD4B expression, we examined mRNA and protein expression in mesenteric arteries treated with normal glucose or high glucose conditions at different time points. RT-qPCR analysis revealed a significant increase in C2CD4B mRNA expression after 3 h of high glucose treatment compared to the normal glucose group, peaking at 6 h post treatment (Figure 1A). While exposure of mesenteric arteries to high glucose for 3 h had no effect on C2CD4B protein expression compared to the normal glucose group, C2CD4B protein was significantly induced after 6 hours of high glucose treatment (Figure 1B).

Interestingly, siRNA-mediated knockdown of C2CD4B prevented the reduction in endothelium-dependent vasodilation induced by 6 h of high glucose in mice mesenteric arteries (Figure 1C). Genetic inhibition of C2CD4B severely blunted increased ROS [dihydroethidium (DHE) cryostaining] and nitric oxide loss [diaminofluorescein-diacetate (DAF-FM)] induced by hyperglycemic conditions in mesenteric arteries (Figure 1D,E). These findings suggest a potential contribution to the development of diabetes-associated vascular complications.

#### 3.2. C2CD4B Evokes Endothelial Dysfunction of Mice Resistance Arteries through a ROS-Dependent Mechanism

To eliminate confounding factors associated with hyperglycemic conditions, we conducted ex vivo studies to evaluate whether C2CD4B protein alone could influence endothelial function. Vascular reactivity studies were performed on precontracted mice mesenteric arteries exposed to the recombinant C2CD4B protein. While 25 and 50 ng/mL did not significantly influence endothelial function, 100 ng/mL induced a significant reduction of acetylcholine-evoked vasorelaxation. A similar result was observed in the presence of 200 ng/mL of C2CD4B. As we noted a prominent impairment in vascular reactivity after incubation with 100 ng/mL of C2CD4B for 1 h (Figure 2A), we decided to use this experimental setting for all subsequent experiments. The experimental setup for assessment of the effects of recombinant C2CD4B is reported in the Supplementary Data, Figure S1. Notably, this effect was markedly prevented by pretreatment with the antioxidant agent Tempol (Figure 2B), highlighting the crucial role of increased ROS generation in C2CD4B-evoked endothelial dysfunction.

To assess the specific endothelial effects of C2CD4B, we focused our attention on isolated human umbilical vein endothelial cells (HUVECs). C2CD4B significantly increased oxidative stress production after 1 h of exposure (Figure 2C). Additionally, the lucigenin-enhanced chemiluminescence assay clearly indicated the specific involvement of the nicotinamide adenine dinucleotide phosphate (NADPH)-dependent oxidase family in mediating superoxide radical ( $O_2^-$ ) generation in response to C2CD4B treatment (Figure 2D).

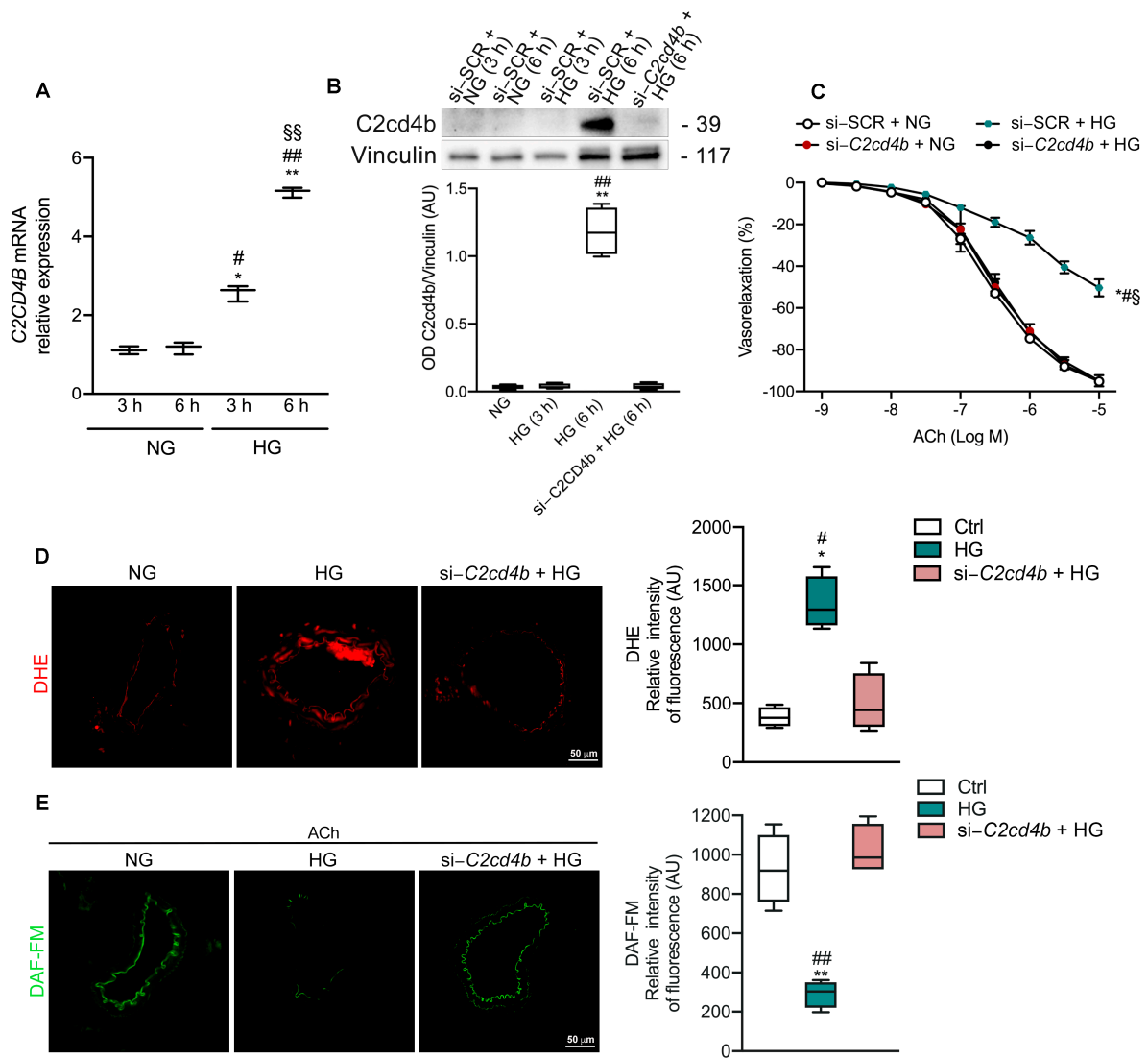


**Figure 1.** Effect of C2CD4B gene silencing on mice mesenteric arteries exposed to hyperglycemic conditions. **(A)** mRNA expression of C2CD4B determined by quantitative reverse transcription polymerase chain reaction in mice mesenteric arteries treated at different time points (3, 6 h) under normal glucose (NG, 5 mM) or high glucose conditions (HG, 30 mM); ( $n = 3$ ). **(B)** Representative western blot and densitometric analyses evaluating protein levels of C2CD4B in mice mesenteric arteries treated with normal glucose (NG) or high glucose (HG) at different time points (3, 6 h), pretransfected with either scramble siRNA (NG 3 h; NG 6 h; HG 3 h and HG 6 h), or specific siRNA against C2CD4B (Si-C2CD4B) before HG 6 h; ( $n = 4$ ). Non-parametric Kruskal–Wallis test with Dunn’s correction was used. **(C)** Acetylcholine (ACh)–evoked vasorelaxation in mice mesenteric arteries exposed to NG or HG conditions and pretransfected with siRNA against C2CD4B (Si-C2CD4B) or scrambled siRNA (Si-SCR); ( $n = 3$ ). **(D)** ROS levels were detected by DHE in mice mesenteric arteries treated with normal glucose (NG), high glucose (HG) alone, or pretransfected with siRNA against C2CD4B (Si-C2CD4B). Box plots show relative fluorescence intensity, (AU, arbitrary units); ( $n = 4$ ). **(E)** NO levels were detected by DAF-FM in mice mesenteric arteries treated with normal glucose (NG), high glucose (HG) alone, or pretransfected with siRNA against C2CD4B (Si-C2CD4B). Box plots show relative fluorescence intensity, (AU, arbitrary units); ( $n = 4$ ). Unless otherwise stated, statistical analyses were performed using one-way or two-way ANOVA followed by Bonferroni post-hoc test. \*  $p < 0.05$ ; \*\*  $p < 0.01$ ; #  $p < 0.05$ ; ##  $p < 0.01$ ; §  $p < 0.05$ ; §§  $p < 0.01$ .

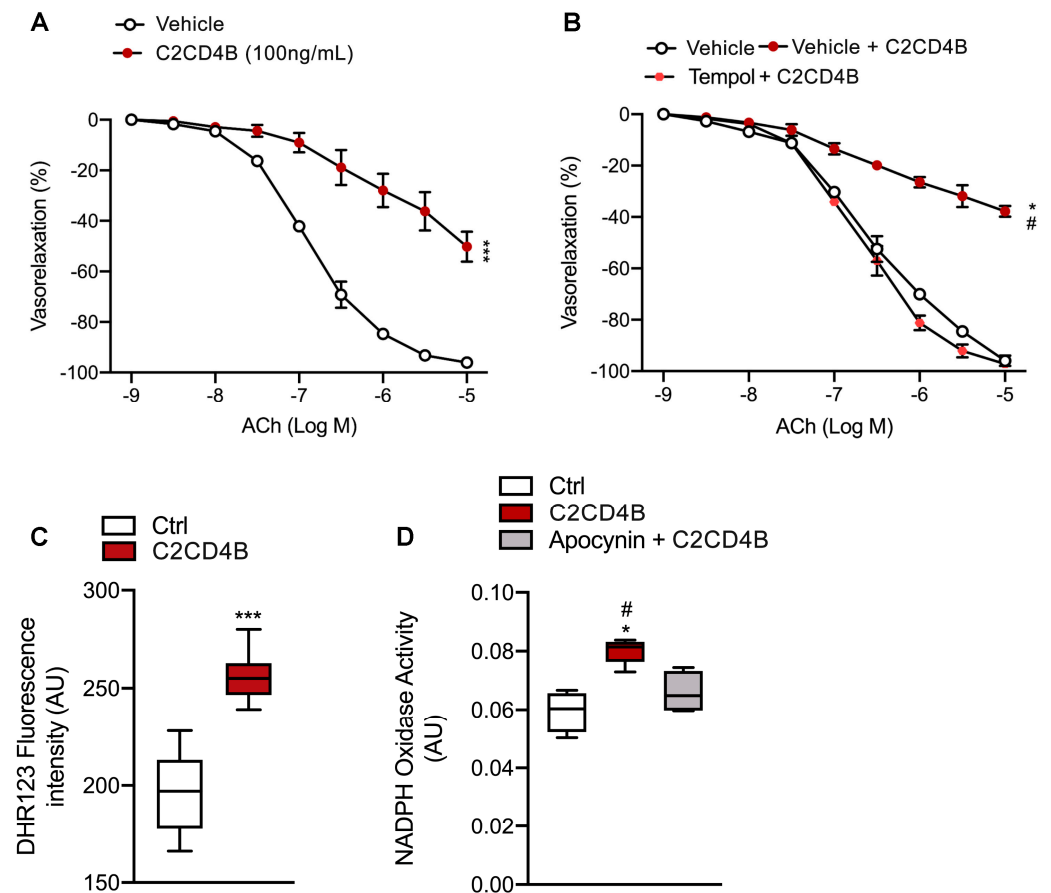


**Figure 2.** Effect of recombinant C2CD4B on mice mesenteric arteries and human EC. (A) Acetylcholine (ACh)-evoked vasorelaxation in mice mesenteric arteries exposed to vehicle or recombinant C2CD4B; ( $n = 3$ ). (B) Acetylcholine (ACh)-evoked vasorelaxation in mice mesenteric arteries exposed to vehicle or recombinant C2CD4B in presence or absence of the antioxidant agent tempol; ( $n = 3$ ). (C) Cellular ROS levels assessed by determining dihydrorhodamine 123 (DHR) fluorescence intensity (AU, arbitrary units); ( $n = 4-6$ ). (D) NADPH-induced lucigenin chemiluminescence (data are expressed as increase in chemiluminescence per minute in arbitrary units) in HUVECs treated with 100 ng/mL of C2CD4B for 1 h; ( $n = 4-6$ ). Statistical analyses were performed using Student's *t*-test, one-way or two-way ANOVA followed by Bonferroni post-hoc test. \*  $p < 0.05$ ; \*\*\*  $p < 0.001$ ; #  $p < 0.05$ .

### 3.3. C2CD4B Relies on PI3K/AKT Pathway to Induce Endothelial Dysfunction of Mice Mesenteric Arteries

Previous mechanistic studies have shown that under hyperglycemic conditions, EC undergo oxidative stress overproduction and apoptosis through a phosphoinositide 3-kinase (PI3K)/Akt-dependent pathway [28]. Compared to control cells, exposure of HUVECs to 1 h of recombinant C2CD4B significantly increased the expression of phosphorylated forms of PI3K and Akt (Figure 3A,B), indicating the involvement of a PI3K signaling pathway. To clarify this issue, subsequent studies were performed in the presence of the pharmacological inhibitors of PI3K and Akt—wortmannin, and Akt inhibitor X, respectively. Interestingly, both the inhibitors prevented increased NADPH oxidase activation in HUVECs (Figure 3C). At the functional level, wortmannin markedly prevented the impairment of endothelial-dependent vasorelaxation as well as the NO reduction observed in C2CD4B-stimulated mesenteric arteries (Figure 3D,E). This effect was also observed after the pretreatment of vessels with the Akt inhibitor X (Figure 3F), clearly indicating the ability of C2CD4B to drive the activation of the PI3K/Akt signaling cascade, leading to excessive ROS generation and, in turn, to endothelial dysfunction.

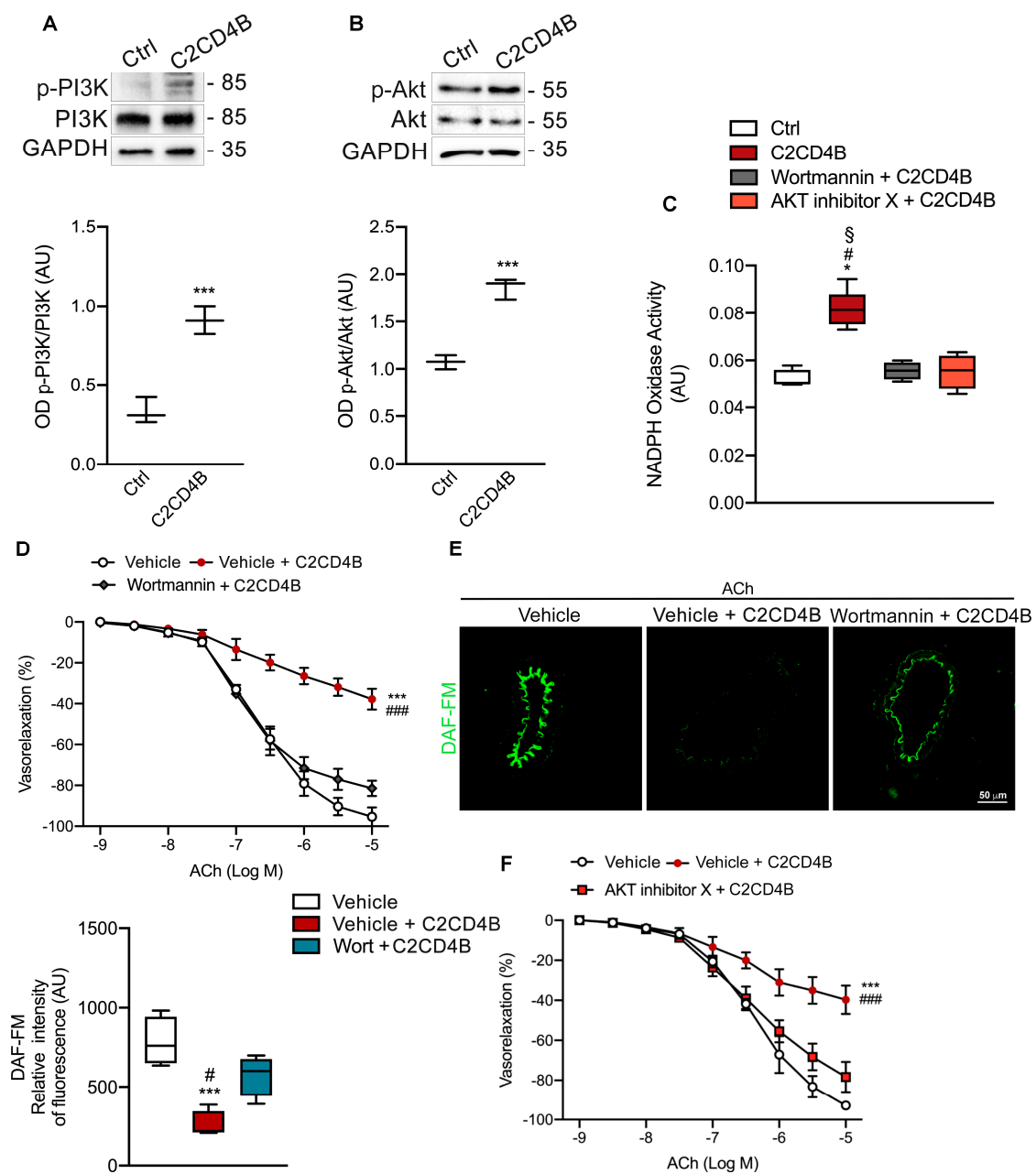


**Figure 3.** C2CD4B promotes endothelial dysfunction of mice mesenteric arteries through PI3K/Akt signaling pathway. (A,B) Representative western blot and densitometric analyses of three independent experiments evaluating protein levels of (A) phospho-PI3K and (B) phospho-Akt protein expression in HUVECs treated with vehicle (ctrl), or recombinant C2CD4B. (C) NADPH-induced lucigenin chemiluminescence (data are expressed as increase in chemiluminescence per minute in arbitrary units) in HUVECs treated with 100 ng/mL of C2CD4B in the presence or absence of wortmannin, or AKT inhibitor X; ( $n = 4-5$ ). (D) Acetylcholine (ACh)-evoked vasorelaxation in mice mesenteric arteries exposed to vehicle or recombinant C2CD4B in the presence or absence of wortmannin ( $n = 3$ ). (E) NO detection by DAF-FM in mice mesenteric arteries treated with vehicle, C2CD4B alone, or pre-treated with wortmannin. Box plot shows relative fluorescence intensity; ( $n = 3$ ). (F) ACh-evoked vasorelaxation in mice mesenteric arteries exposed to vehicle or recombinant C2CD4B in the presence or absence of AKT inhibitor X; ( $n = 3$ ). Statistical analyses were performed using Student's *t*-test, one-way or two-way ANOVA followed by Bonferroni post-hoc test. \*  $p < 0.05$ ; \*\*\*  $p < 0.001$ ; #  $p < 0.05$ ; §  $p < 0.05$ ; ###  $p < 0.001$ .

### 3.4. Inhibition of Endothelial Nitric Oxide Synthase Prevents C2CD4B-Mediated ROS Generation

To determine whether the enhanced superoxide formation was dependent on uncoupled eNOS, C2CD4B-treated HUVECs were pre-incubated with the NOS inhibitor, N- $\omega$ -nitro-L-arginine methyl ester (L-NAME). Intracellular superoxide production was evaluated using dihydroethidium (DHE) cryostaining in mesenteric arteries. We found that the C2CD4B-induced increase in intracellular superoxide generation was markedly inhibited by L-NAME pre-treatment (Figure 4), suggesting the involvement of eNOS uncoupling in the exaggerated ROS production in response to C2CD4B.

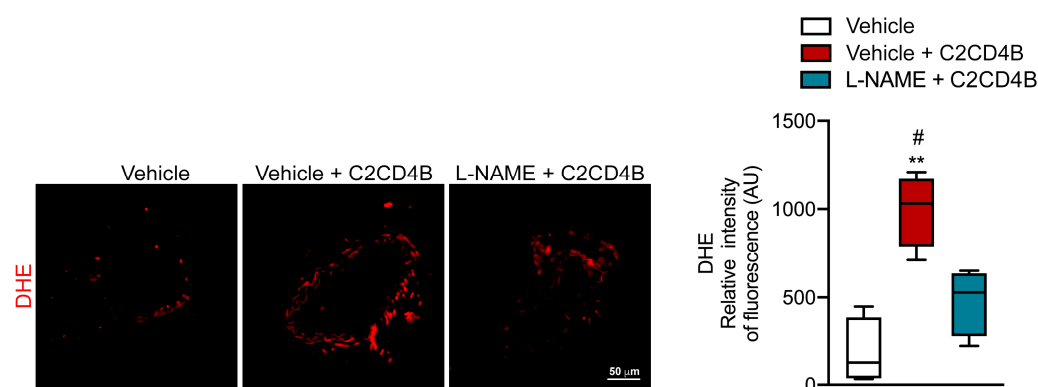


**Figure 4.** C2CD4B induces eNOS uncoupling in mesenteric arteries. ROS production detected by DHE in mice mesenteric arteries treated with vehicle, C2CD4B alone, or pre-treated with L-NAME. Box plot shows relative fluorescence intensity; ( $n = 4$ ). Statistical analyses were performed using one-way ANOVA followed by Bonferroni post-hoc test. \*\*  $p < 0.01$ , #  $p < 0.05$ .

### 3.5. C2CD4B-Mediated eNOS Uncoupling Prevented by PI3K Inhibition

Given the critical role of the dimeric form of eNOS in its functionality [29], we investigated the proportion of the enzyme existing as either dimer or monomer in HUVECs treated with recombinant C2CD4B. Exposure of HUVECs to recombinant C2CD4B for 1 h markedly reduced the dimer/monomer ratio of eNOS compared to control cells, while increasing phosphorylation of eNOS at Thr495, an inhibitory site (Figure 5A,B). Intriguingly, these effects were significantly mitigated by wortmannin pre-treatment (Figure 5A,B; Supplementary Data, Figure S2), indicating the involvement of PI3K in C2CD4B-mediated eNOS uncoupling.

### 3.6. C2CD4B Induces eNOS Uncoupling and Vascular Dysfunction via a PI3K/Akt/PKC $\alpha$ Signaling Cascade

To further explore the potential role of protein kinase C (PKC), a family of kinases activated in response to high glucose concentration to induce oxidative stress [30]. In particular, we focused our attention on PKC $\alpha$ , known to induce eNOS phosphorylation on its inhibitory site [31]. In addition, PKC upregulation has been reported in metabolic disorders, including diabetes [32].

Recombinant C2CD4B markedly upregulated the protein expression of phosphorylated PKC $\alpha$ , an effect prevented by wortmannin pre-treatment (Figure 6A). As PKC $\beta$  is not expressed in HUVECs, Go6976, a specific PKC $\alpha$  pharmacological inhibitor, was employed [33]. Go6976 prevented C2CD4B-induced eNOS dysfunction, as indicated by the preservation of eNOS dimerization (Figure 6B). These findings strongly support the notion that PKC $\alpha$  participates in the C2CD4B cascade, acting downstream of PI3K to mediate uncoupling of eNOS. At the functional level, experiments on mesenteric arteries were conducted, assessing the vascular effects of Go6976 pre-treatment against C2CD4B-induced endothelial dysfunction. Consistent with molecular level observations, Go6976 significantly attenuated endothelial dysfunction, as well as the increased vasoconstriction induced by C2CD4B (Figure 6C,D), clearly indicating the crucial role of PKC $\alpha$  in its harmful effect.

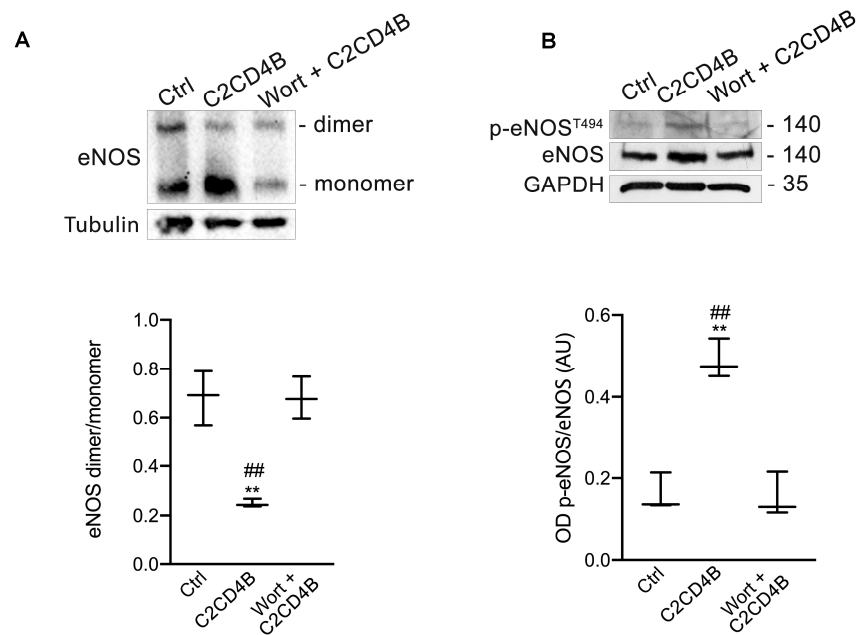


**Figure 5.** Wortmannin prevents C2CD4B-induced eNOS uncoupling in EC. **(A)** Representative western blot and densitometric analyses of three independent experiments evaluating eNOS dimer (280 kDa) and eNOS monomer (140 kDa) protein expression in HUVECs treated with vehicle (ctrl), recombinant C2CD4B alone, or pre-treated with wortmannin. Dimer/monomer eNOS were examined by non-reducing low-temperature SDS-PAGE. **(B)** Representative western blot and densitometric analyses of three independent experiments evaluating protein levels of phosphorylated eNOS at Thr 495 (p-eNOS<sup>T495</sup>), and total eNOS expression in HUVECs treated with vehicle (ctrl), recombinant C2CD4B alone, or pre-treated with wortmannin. Statistical analyses were performed using one-way ANOVA followed by Bonferroni post-hoc test. \*\*  $p < 0.001$ ; ###  $p < 0.001$ .

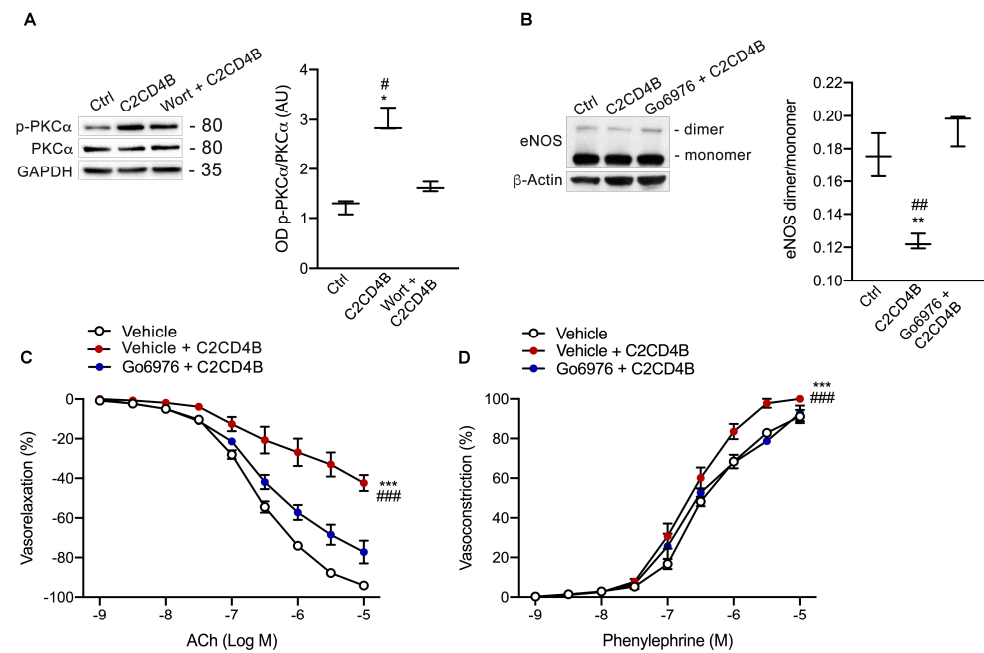


**Figure 6.** Pharmacological inhibition of PKC $\alpha$  reverses eNOS uncoupling and prevents vascular dysfunction induced by C2CD4B. **(A)** Representative western blot and densitometric analyses of 3 independent experiments evaluating the expression of phosphorylated form PKC $\alpha$  in HUVECs treated with vehicle (ctrl), recombinant C2CD4B alone, or pre-treated with wortmannin. **(B)** Representative western blot and densitometric analyses of three independent experiments evaluating the expression of phosphorylated eNOS at Thr 495 (p-eNOS<sup>T495</sup>) and total eNOS expression in HUVECs treated with vehicle (ctrl), recombinant C2CD4B alone, or pre-treated with Go6976. **(C)** Dose-dependent vasorelaxation to ACh in HUVECs treated with vehicle (ctrl), recombinant C2CD4B alone, or pre-treated with Go6976. **(D)** Dose-dependent vasoconstriction to Phenylephrine in HUVECs treated with vehicle (ctrl), recombinant C2CD4B alone, or pre-treated with Go6976. Statistical analyses were performed using one-way ANOVA followed by Bonferroni post-hoc test. \*\*  $p < 0.001$ ; ###  $p < 0.001$ ; \*\*\*\*  $p < 0.0001$ ; #####  $p < 0.00001$ .

western blot and densitometric analyses of three independent experiments evaluating eNOS dimer (280 kDa) and eNOS monomer (140 kDa) protein expression in HUVECs treated with vehicle (ctrl), recombinant C2CD4B alone, or pre-treated with the pharmacological inhibitor of PKC $\alpha$ , Go6976. Dimer/monomer eNOS were examined by non-reducing low-temperature SDS-PAGE. (C) Acetylcholine (ACh)-evoked vasorelaxation in mice mesenteric arteries exposed to vehicle or recombinant C2CD4B in the presence or absence of the PKC $\alpha$  inhibitor, Go6976; ( $n = 3-4$ ). (D) Dose-response curves to phenylephrine of mice mesenteric arteries exposed to vehicle or recombinant C2CD4B in the presence or absence of Go6976; ( $n = 3-4$ ). Statistical analyses were performed using one-way or two-way ANOVA followed by Bonferroni post-hoc test. \*  $p < 0.05$ ; \*\*  $p < 0.01$ , \*\*\*  $p < 0.001$ ; #  $p < 0.05$ ; ##  $p < 0.01$ ; ###  $p < 0.001$ .

#### 4. Discussion

Oxidative stress is a major trigger for diabetes mellitus-induced vascular endothelial dysfunction leading to a reduction in NO bioavailability [34]. There is overwhelming evidence that endothelial dysfunction plays a role in the progression of vascular and end-organ damage in diabetic patients. This makes it a crucial early target for preventing cardiovascular diseases [34]. Diabetes leads to multiple comorbidities, such as heart disease, kidney dysfunction, retinopathy, and impaired wound healing. All these issues can be attributed to vascular disease initiated by the loss of endothelial barrier integrity [35].

Originally described by Warton et al. [12], C2CD4B was, compared to smooth muscle cells and fibroblasts, predominantly identified in human endothelial cells. It was found to be induced after 2 h of treatment with IL-1 $\beta$ .

Genome-wide association studies revealed that single nucleotide polymorphisms (SNPs) in close proximity to the VPS13C, C2CD4A, and C2CD4B genes on chromosome 15q contribute to an increased risk of type 2 diabetes [14,19]. Through human pancreatic islet expression quantitative trait loci (eQTL) analysis, the T2DM-associated risk variant rs7163757 was reported to be linked to increased expression of C2CD4B in alpha cells [15]. However, it remains unknown whether C2CD4B is affected by hyperglycemia conditions and mediates vascular damage in this context.

Here, we show that high glucose markedly increased both mRNA and protein expression of C2CD4B in mice mesenteric arteries in a time-dependent manner. More importantly, the knockdown of C2CD4B protects against high glucose-induced oxidative stress and endothelial dysfunction.

Our findings indicate that C2CD4B is up-regulated by high glucose levels and its inhibition prevents oxidative stress in human endothelial cells and in mice mesenteric arteries.

In diabetic blood vessels, major sources of ROS include the mitochondrial electron transport chain, nicotinamide dinucleotide phosphate (NADPH) oxidase, xanthine oxidase (XO) and uncoupled endothelial nitric oxide synthase (eNOS) [36]. In our study, the increase in ROS generation can, in part, be ascribed to an enhanced expression of NADPH oxidase activity observed in EC treated with the recombinant C2CD4B. Under high glucose conditions, aberrant activation of eNOS, referred to as eNOS uncoupling, produces O $_2^-$  instead of NO. This superoxide rapidly combines with vascular NO to form peroxynitrite (ONOO $-$ ), reducing the bioavailability of NO in vascular EC. This phenomenon results in a vicious cycle that continuously increases superoxide in blood vessels and ultimately impairs endothelium [37]. Importantly, uncoupling of eNOS has also been observed in diabetic patients with endothelial dysfunction [38]. In our experimental setting, an additional contribution to superoxide production came from uncoupled eNOS since pre-treatment with the NOS inhibitor markedly reduced C2CD4B-induced ROS production. Although activation of the PI3K/Akt pathway is critical for maintaining vascular tone and endothelial integrity [39,40], previous studies by Sheu et al. [28] reported that, via a PI3K/Akt-dependent pathway, hyperglycemic conditions may cause ROS generation in HUVECs.

Consistent with these findings, the results of the present study demonstrate that activation of the PI3K/Akt-signaling pathway by C2CD4B can significantly induce oxidative stress in EC and evoke endothelial dysfunction in ex vivo-treated mesenteric arteries.

These findings are supported by functional and molecular studies performed on mesenteric arteries, showing that the pharmacological inhibition of PI3K/Akt activity can prevent impaired endothelium-dependent relaxation as well as the reduction of NO levels observed after exposure of vessels to recombinant C2CD4B.

We also observed that C2CD4B exposure in HUVECs resulted in a marked PI3K-dependent reduction in eNOS dimerization and increased phosphorylation of the enzyme on the inhibitory site T495. These are indicative of uncoupled eNOS [41,42]. Moreover, increased eNOS phosphorylation at T495 has been reported to down-regulate NO production [43,44].

Protein kinase C (PKC), an intracellular family of serine/threonine protein kinases, has a crucial role in numerous biological processes, including proliferation, survival, invasion, migration, and apoptosis [45,46].

In addition to being associated with several vascular disorders, including hypertension, coronary artery disease, and diabetic vasculopathy [47], activation of PKC has emerged as an important mechanism regulating endothelial dysfunction in diabetes mellitus [48]. In vitro, high glucose concentrations activate PKC and increase superoxide production [49]. Several studies have also demonstrated the ability of PKC to specifically phosphorylate eNOS at T495, inducing oxidative stress and reducing eNOS catalytic activity [31,48]. These concepts are supported by preclinical and clinical studies demonstrating that pharmacological inhibition of PKC ameliorates vascular complications caused by hyperglycemia [50,51].

Our results further show that C2CD4B causes activation of PKC $\alpha$  in HUVEC cells, an effect blunted by PI3K inhibition. We also observed that the PKC $\alpha$  inhibitor Go6976 prevented the decrease in eNOS dimer/monomer ratio, clearly indicating on the one hand, PKC $\alpha$  as a downstream effector of the PI3K/Akt pathway, and an upstream mediator of eNOS uncoupling on the other. These results are consistent with those of previous studies demonstrating the role of PKC activation in mediating eNOS uncoupling and oxidative stress in EC [31]. These data were further corroborated by functional studies, which revealed that pharmacological inhibition of PKC $\alpha$  resulted in significant protection against C2CD4B-induced vascular dysfunction. An exciting observation emerging from our study is that Go6976 did not completely restore endothelium-dependent vasorelaxation, but completely prevented vasoconstriction induced by C2CD4B in mesenteric arteries. These results could be explained by the opposite effects that PKC may elicit on vascular districts. Indeed, PKC is known to influence both vascular relaxation and contraction [52]. For instance, it may mediate NO synthesis but could also induce the release of endothelium-derived constricting factors, thus promoting vasoconstriction [53].

Our data support the notion that C2CD4B is a negative modulator of vascular PKC function and may represent a potential target in vascular disorders. In detail, via PKC $\alpha$ , C2CD4B induces vascular dysfunction through (i) an impairment of endothelium-dependent vasodilation, and (ii) an enhancement of vascular contraction.

Although newly generated PKC inhibitors have shown promise in the treatment of macular edema [54], retinopathy [55], and microvascular complications [56] in diabetic patients, targeting upstream activators could be a therapeutic strategy for the development of inhibitors able to prevent or delay vascular complications in the early stages of diabetes mellitus.

## 5. Conclusions

Here we present, for the first time, evidence demonstrating that hyperglycemia increased mRNA expression of the diabetic-associated protein C2CD4B. Mechanistically, via activation of the PI3K/Akt/PKC $\alpha$ -pathway, C2CD4B promotes oxidative stress-dependent endothelial dysfunction, driving eNOS uncoupling and NADPH oxidase dysregulation.

These findings lay the groundwork for further research aimed at deepening our understanding of the molecular mechanism underlying the role of C2CD4B in cardiovascular diseases. Additionally, they suggest the potential therapeutic value of targeting

this protein for the prevention of oxidative stress in diabetes mellitus-induced vascular endothelial dysfunction.

**Supplementary Materials:** The following supporting information can be downloaded at: <https://www.mdpi.com/article/10.3390/antiox13010101/s1>, Figure S1: Experimental setup for the assessment of the effects of recombinant C2CD4B on mice mesenteric arteries; Figure S2: Effect of incubation of cell lysates from endothelial cells in the presence or the absence of the reducing agent  $\beta$ -mercaptoethanol (1.5%, 2.5%) on levels of endothelial nitric oxide synthase (eNOS). Reference [57] are cited in the supplementary materials.

**Author Contributions:** Conceptualization: P.D.P., C.V. and A.C.; investigation: P.D.P., A.C.A., V.P., A.D. and E.V.; methodology: P.D.P., A.C.A., V.P., A.D., E.V. and M.R.R.; data curation: P.D.P., A.C., A.C.A., V.P., C.I. and V.V.; writing—original draft preparation: P.D.P. and A.C.; review and editing: M.C., C.V. and A.C. All authors have read and agreed to the published version of the manuscript.

**Funding:** This research was funded by PRIN 2020 to CV (2020YRETTX, Italian Ministry of University and Research).

**Institutional Review Board Statement:** The study was conducted according to the guidelines of the Declaration of Helsinki, and approved by the Ethical Committee for Animal Studies of the Istituto Neurologico Mediterraneo IRCCS Neuromed (Ethical protocol code: 570/2019PR).

**Informed Consent Statement:** Not applicable.

**Data Availability Statement:** The data presented in this study are available on request from the corresponding author.

**Conflicts of Interest:** The authors declare no conflicts of interest.

## References

1. NCD Risk Factor Collaboration (NCD-RisC). Worldwide trends in diabetes since 1980: A pooled analysis of 751 population-based studies with 4.4 million participants. *Lancet* **2016**, *387*, 1513–1530. [[CrossRef](#)] [[PubMed](#)]
2. Saeedi, P.; Petersohn, I.; Salpea, P.; Malanda, B.; Karuranga, S.; Unwin, N.; Colagiuri, S.; Guariguata, L.; Motala, A.A.; Ogurtsova, K.; et al. Global and regional diabetes prevalence estimates for 2019 and projections for 2030 and 2045: Results from the International Diabetes Federation Diabetes Atlas, 9(th) edition. *Diabetes Res. Clin. Pract.* **2019**, *157*, 107843. [[CrossRef](#)] [[PubMed](#)]
3. Rask-Madsen, C.; King, G.L. Vascular complications of diabetes: Mechanisms of injury and protective factors. *Cell Metab.* **2013**, *17*, 20–33. [[CrossRef](#)] [[PubMed](#)]
4. Schiattarella, G.G.; Carrizzo, A.; Icardi, F.; Damato, A.; Ambrosio, M.; Madonna, M.; Trimarco, V.; Marino, M.; De Angelis, E.; Settembrini, S.; et al. Rac1 Modulates Endothelial Function and Platelet Aggregation in Diabetes Mellitus. *J. Am. Heart Assoc.* **2018**, *7*, e007322. [[CrossRef](#)]
5. Carrizzo, A.; Izzo, C.; Oliveti, M.; Alfano, A.; Virtuoso, N.; Capunzo, M.; Di Pietro, P.; Calabrese, M.; De Simone, E.; Sciarretta, S.; et al. The Main Determinants of Diabetes Mellitus Vascular Complications: Endothelial Dysfunction and Platelet Hyperaggregation. *Int. J. Mol. Sci.* **2018**, *19*, 2968. [[CrossRef](#)] [[PubMed](#)]
6. Sena, C.M.; Pereira, A.M.; Seica, R. Endothelial dysfunction—A major mediator of diabetic vascular disease. *Biochim. Biophys. Acta* **2013**, *1832*, 2216–2231. [[CrossRef](#)]
7. Muniyappa, R.; Sowers, J.R. Role of insulin resistance in endothelial dysfunction. *Rev. Endocr. Metab. Disord.* **2013**, *14*, 5–12. [[CrossRef](#)]
8. Hadi, H.A.; Suwaidi, J.A. Endothelial dysfunction in diabetes mellitus. *Vasc. Health Risk Manag.* **2007**, *3*, 853–876.
9. Cines, D.B.; Pollak, E.S.; Buck, C.A.; Loscalzo, J.; Zimmerman, G.A.; McEver, R.P.; Pober, J.S.; Wick, T.M.; Konkle, B.A.; Schwartz, B.S.; et al. Endothelial cells in physiology and in the pathophysiology of vascular disorders. *Blood* **1998**, *91*, 3527–3561.
10. Cai, Z.; Yuan, S.; Zhong, Y.; Deng, L.; Li, J.; Tan, X.; Feng, J. Amelioration of Endothelial Dysfunction in Diabetes: Role of Takeda G Protein-Coupled Receptor 5. *Front. Pharmacol.* **2021**, *12*, 637051. [[CrossRef](#)]
11. Ogaki, S.; Harada, S.; Shiraki, N.; Kume, K.; Kume, S. An expression profile analysis of ES cell-derived definitive endodermal cells and Pdx1-expressing cells. *BMC Dev. Biol.* **2011**, *11*, 13. [[CrossRef](#)]
12. Warton, K.; Foster, N.C.; Gold, W.A.; Stanley, K.K. A novel gene family induced by acute inflammation in endothelial cells. *Gene* **2004**, *342*, 85–95. [[CrossRef](#)]
13. Sabater-Lleal, M.; Huffman, J.E.; de Vries, P.S.; Marten, J.; Mastrangelo, M.A.; Song, C.; Pankratz, N.; Ward-Caviness, C.K.; Yanek, L.R.; Trompet, S.; et al. Genome-Wide Association Transethnic Meta-Analyses Identifies Novel Associations Regulating Coagulation Factor VIII and von Willebrand Factor Plasma Levels. *Circulation* **2019**, *139*, 620–635. [[CrossRef](#)]

14. Yamauchi, T.; Hara, K.; Maeda, S.; Yasuda, K.; Takahashi, A.; Horikoshi, M.; Nakamura, M.; Fujita, H.; Grarup, N.; Cauchi, S.; et al. A genome-wide association study in the Japanese population identifies susceptibility loci for type 2 diabetes at UBE2E2 and C2CD4A–C2CD4B. *Nat. Genet.* **2010**, *42*, 864–868. [[CrossRef](#)]
15. Kycia, I.; Wolford, B.N.; Huyghe, J.R.; Fuchsberger, C.; Vadlamudi, S.; Kursawe, R.; Welch, R.P.; Albanus, R.D.; Uyar, A.; Khetan, S.; et al. A Common Type 2 Diabetes Risk Variant Potentiates Activity of an Evolutionarily Conserved Islet Stretch Enhancer and Increases C2CD4A and C2CD4B Expression. *Am. J. Hum. Genet.* **2018**, *102*, 620–635. [[CrossRef](#)]
16. Cui, B.; Zhu, X.; Xu, M.; Guo, T.; Zhu, D.; Chen, G.; Li, X.; Xu, L.; Bi, Y.; Chen, Y.; et al. A genome-wide association study confirms previously reported loci for type 2 diabetes in Han Chinese. *PLoS ONE* **2011**, *6*, e22353. [[CrossRef](#)]
17. Shu, X.O.; Long, J.; Cai, Q.; Qi, L.; Xiang, Y.B.; Cho, Y.S.; Tai, E.S.; Li, X.; Lin, X.; Chow, W.H.; et al. Identification of new genetic risk variants for type 2 diabetes. *PLoS Genet.* **2010**, *6*, e1001127. [[CrossRef](#)]
18. DIAbetes Genetics Replication And Meta-analysis (DIAGRAM) Consortium; Asian Genetic Epidemiology Network Type 2 Diabetes (AGEN-T2D) Consortium; South Asian Type 2 Diabetes (SAT2D) Consortium; Mexican American Type 2 Diabetes (MAT2D) Consortium; Type 2 Diabetes Genetic Exploration by Next-generation sequencing in multi-Ethnic Samples (T2D-GENES) Consortium; Mahajan, A.; Go, M.J.; Zhang, W.; Below, J.E.; Gaulton, K.J.; et al. Genome-wide trans-ancestry meta-analysis provides insight into the genetic architecture of type 2 diabetes susceptibility. *Nat. Genet.* **2014**, *46*, 234–244. [[CrossRef](#)]
19. Grarup, N.; Overvad, M.; Sparso, T.; Witte, D.R.; Pisinger, C.; Jorgensen, T.; Yamauchi, T.; Hara, K.; Maeda, S.; Kadowaki, T.; et al. The diabetogenic VPS13C/C2CD4A/C2CD4B rs7172432 variant impairs glucose-stimulated insulin response in 5,722 non-diabetic Danish individuals. *Diabetologia* **2011**, *54*, 789–794. [[CrossRef](#)] [[PubMed](#)]
20. Ingelsson, E.; Langenberg, C.; Hivert, M.F.; Prokopenko, I.; Lyssenko, V.; Dupuis, J.; Magi, R.; Sharp, S.; Jackson, A.U.; Assimes, T.L.; et al. Detailed physiologic characterization reveals diverse mechanisms for novel genetic Loci regulating glucose and insulin metabolism in humans. *Diabetes* **2010**, *59*, 1266–1275. [[CrossRef](#)] [[PubMed](#)]
21. Dupuis, J.; Langenberg, C.; Prokopenko, I.; Saxena, R.; Soranzo, N.; Jackson, A.U.; Wheeler, E.; Glazer, N.L.; Bouatia-Naji, N.; Gloyn, A.L.; et al. New genetic loci implicated in fasting glucose homeostasis and their impact on type 2 diabetes risk. *Nat. Genet.* **2010**, *42*, 105–116. [[CrossRef](#)] [[PubMed](#)]
22. Strawbridge, R.J.; Dupuis, J.; Prokopenko, I.; Barker, A.; Ahlqvist, E.; Rybin, D.; Petrie, J.R.; Travers, M.E.; Bouatia-Naji, N.; Dimas, A.S.; et al. Genome-wide association identifies nine common variants associated with fasting proinsulin levels and provides new insights into the pathophysiology of type 2 diabetes. *Diabetes* **2011**, *60*, 2624–2634. [[CrossRef](#)] [[PubMed](#)]
23. Boesgaard, T.W.; Grarup, N.; Jorgensen, T.; Borch-Johnsen, K.; Meta-Analysis of, G.; Insulin-Related Trait, C.; Hansen, T.; Pedersen, O. Variants at DGKB/TMEM195, ADRA2A, GLIS3 and C2CD4B loci are associated with reduced glucose-stimulated beta cell function in middle-aged Danish people. *Diabetologia* **2010**, *53*, 1647–1655. [[CrossRef](#)] [[PubMed](#)]
24. Schiattarella, G.G.; Cattaneo, F.; Carrizzo, A.; Paolillo, R.; Boccella, N.; Ambrosio, M.; Damato, A.; Pironti, G.; Franzone, A.; Russo, G.; et al. Akap1 Regulates Vascular Function and Endothelial Cells Behavior. *Hypertension* **2018**, *71*, 507–517. [[CrossRef](#)] [[PubMed](#)]
25. Di Pietro, P.; Carrizzo, A.; Sommella, E.; Olivetti, M.; Iacoviello, L.; Di Castelnuovo, A.; Acernese, F.; Damato, A.; De Lucia, M.; Merciai, F.; et al. Targeting the ASase/S1P pathway protects from sortilin-evoked vascular damage in hypertension. *J. Clin. Invest.* **2022**, *132*, e146343. [[CrossRef](#)] [[PubMed](#)]
26. Di Pietro, P.; Lizio, R.; Izzo, C.; Visco, V.; Damato, A.; Venturini, E.; De Lucia, M.; Galasso, G.; Migliarino, S.; Rasile, B.; et al. A Novel Combination of High-Load Omega-3 Lysine Complex (AvailOm((R))) and Anthocyanins Exerts Beneficial Cardiovascular Effects. *Antioxidants* **2022**, *11*, 896. [[CrossRef](#)] [[PubMed](#)]
27. Carrizzo, A.; Iside, C.; Nebbioso, A.; Carafa, V.; Damato, A.; Sciarretta, S.; Frati, G.; Di Nonno, F.; Valenti, V.; Ciccarelli, M.; et al. SIRT1 pharmacological activation rescues vascular dysfunction and prevents thrombosis in MTHFR deficiency. *Cell Mol. Life Sci.* **2022**, *79*, 410. [[CrossRef](#)]
28. Sheu, M.L.; Ho, F.M.; Yang, R.S.; Chao, K.F.; Lin, W.W.; Lin-Shiau, S.Y.; Liu, S.H. High glucose induces human endothelial cell apoptosis through a phosphoinositide 3-kinase-regulated cyclooxygenase-2 pathway. *Arterioscler. Thromb. Vasc. Biol.* **2005**, *25*, 539–545. [[CrossRef](#)]
29. Andrew, P.J.; Mayer, B. Enzymatic function of nitric oxide synthases. *Cardiovasc. Res.* **1999**, *43*, 521–531. [[CrossRef](#)]
30. Lien, C.F.; Chen, S.J.; Tsai, M.C.; Lin, C.S. Potential Role of Protein Kinase C in the Pathophysiology of Diabetes-Associated Atherosclerosis. *Front. Pharmacol.* **2021**, *12*, 716332. [[CrossRef](#)]
31. Chen, F.; Kumar, S.; Yu, Y.; Aggarwal, S.; Gross, C.; Wang, Y.; Chakraborty, T.; Verin, A.D.; Catravas, J.D.; Lucas, R.; et al. PKC-dependent phosphorylation of eNOS at T495 regulates eNOS coupling and endothelial barrier function in response to G+ toxins. *PLoS ONE* **2014**, *9*, e99823. [[CrossRef](#)] [[PubMed](#)]
32. Geraldès, P.; King, G.L. Activation of protein kinase C isoforms and its impact on diabetic complications. *Circ. Res.* **2010**, *106*, 1319–1331. [[CrossRef](#)]
33. Lorenzi, O.; Frieden, M.; Vilemin, P.; Fournier, M.; Foti, M.; Vischer, U.M. Protein kinase C-delta mediates von Willebrand factor secretion from endothelial cells in response to vascular endothelial growth factor (VEGF) but not histamine. *J. Thromb. Haemost.* **2008**, *6*, 1962–1969. [[CrossRef](#)] [[PubMed](#)]
34. Versari, D.; Daghini, E.; Virdis, A.; Ghiadoni, L.; Taddei, S. Endothelial dysfunction as a target for prevention of cardiovascular disease. *Diabetes Care* **2009**, *32* (Suppl 2.), S314–S321. [[CrossRef](#)]
35. Forbes, J.M.; Cooper, M.E. Mechanisms of diabetic complications. *Physiol. Rev.* **2013**, *93*, 137–188. [[CrossRef](#)]

36. An, Y.; Xu, B.T.; Wan, S.R.; Ma, X.M.; Long, Y.; Xu, Y.; Jiang, Z.Z. The role of oxidative stress in diabetes mellitus-induced vascular endothelial dysfunction. *Cardiovasc. Diabetol.* **2023**, *22*, 237. [[CrossRef](#)] [[PubMed](#)]
37. Forstermann, U.; Munzel, T. Endothelial nitric oxide synthase in vascular disease: From marvel to menace. *Circulation* **2006**, *113*, 1708–1714. [[CrossRef](#)]
38. Heitzer, T.; Krohn, K.; Albers, S.; Meinertz, T. Tetrahydrobiopterin improves endothelium-dependent vasodilation by increasing nitric oxide activity in patients with Type II diabetes mellitus. *Diabetologia* **2000**, *43*, 1435–1438. [[CrossRef](#)]
39. Chen, J.; Somanath, P.R.; Razorenova, O.; Chen, W.S.; Hay, N.; Bornstein, P.; Byzova, T.V. Akt1 regulates pathological angiogenesis, vascular maturation and permeability in vivo. *Nat. Med.* **2005**, *11*, 1188–1196. [[CrossRef](#)]
40. Carrizzo, A.; Conte, G.M.; Sommella, E.; Damato, A.; Ambrosio, M.; Sala, M.; Scala, M.C.; Aquino, R.P.; De Lucia, M.; Madonna, M.; et al. Novel Potent Decameric Peptide of *Spirulina platensis* Reduces Blood Pressure Levels Through a PI3K/AKT/eNOS-Dependent Mechanism. *Hypertension* **2019**, *73*, 449–457. [[CrossRef](#)]
41. Luczak, A.; Madej, M.; Kasprzyk, A.; Doroszko, A. Role of the eNOS Uncoupling and the Nitric Oxide Metabolic Pathway in the Pathogenesis of Autoimmune Rheumatic Diseases. *Oxid. Med. Cell Longev.* **2020**, *2020*, 1417981. [[CrossRef](#)] [[PubMed](#)]
42. Thum, T.; Fraccarollo, D.; Schultheiss, M.; Froese, S.; Galuppo, P.; Widder, J.D.; Tsikas, D.; Ertl, G.; Bauersachs, J. Endothelial nitric oxide synthase uncoupling impairs endothelial progenitor cell mobilization and function in diabetes. *Diabetes* **2007**, *56*, 666–674. [[CrossRef](#)] [[PubMed](#)]
43. Lin, M.I.; Fulton, D.; Babbitt, R.; Fleming, I.; Busse, R.; Pritchard, K.A., Jr.; Sessa, W.C. Phosphorylation of threonine 497 in endothelial nitric-oxide synthase coordinates the coupling of L-arginine metabolism to efficient nitric oxide production. *J. Biol. Chem.* **2003**, *278*, 44719–44726. [[CrossRef](#)] [[PubMed](#)]
44. Michell, B.J.; Harris, M.B.; Chen, Z.P.; Ju, H.; Venema, V.J.; Blackstone, M.A.; Huang, W.; Venema, R.C.; Kemp, B.E. Identification of regulatory sites of phosphorylation of the bovine endothelial nitric-oxide synthase at serine 617 and serine 635. *J. Biol. Chem.* **2002**, *277*, 42344–42351. [[CrossRef](#)]
45. Kent, K.C.; Mii, S.; Harrington, E.O.; Chang, J.D.; Mallette, S.; Ware, J.A. Requirement for protein kinase C activation in basic fibroblast growth factor-induced human endothelial cell proliferation. *Circ. Res.* **1995**, *77*, 231–238. [[CrossRef](#)]
46. Kinsella, J.L.; Grant, D.S.; Weeks, B.S.; Kleinman, H.K. Protein kinase C regulates endothelial cell tube formation on basement membrane matrix, Matrigel. *Exp. Cell Res.* **1992**, *199*, 56–62. [[CrossRef](#)]
47. Quagliaro, L.; Picconi, L.; Assaloni, R.; Martinelli, L.; Motz, E.; Ceriello, A. Intermittent high glucose enhances apoptosis related to oxidative stress in human umbilical vein endothelial cells: The role of protein kinase C and NAD(P)H-oxidase activation. *Diabetes* **2003**, *52*, 2795–2804. [[CrossRef](#)]
48. Hink, U.; Li, H.; Mollnau, H.; Oelze, M.; Matheis, E.; Hartmann, M.; Skatchkov, M.; Thaiss, F.; Stahl, R.A.; Warnholtz, A.; et al. Mechanisms underlying endothelial dysfunction in diabetes mellitus. *Circ. Res.* **2001**, *88*, E14–E22. [[CrossRef](#)]
49. Ishii, H.; Koya, D.; King, G.L. Protein kinase C activation and its role in the development of vascular complications in diabetes mellitus. *J. Mol. Med.* **1998**, *76*, 21–31. [[CrossRef](#)]
50. Ishii, H.; Jirousek, M.R.; Koya, D.; Takagi, C.; Xia, P.; Clermont, A.; Bursell, S.E.; Kern, T.S.; Ballas, L.M.; Heath, W.F.; et al. Amelioration of vascular dysfunctions in diabetic rats by an oral PKC beta inhibitor. *Science* **1996**, *272*, 728–731. [[CrossRef](#)]
51. Beckman, J.A.; Goldfine, A.B.; Gordon, M.B.; Garrett, L.A.; Creager, M.A. Inhibition of protein kinase C $\beta$  prevents impaired endothelium-dependent vasodilation caused by hyperglycemia in humans. *Circ. Res.* **2002**, *90*, 107–111. [[CrossRef](#)] [[PubMed](#)]
52. Ringvold, H.C.; Khalil, R.A. Protein Kinase C as Regulator of Vascular Smooth Muscle Function and Potential Target in Vascular Disorders. *Adv. Pharmacol.* **2017**, *78*, 203–301. [[CrossRef](#)] [[PubMed](#)]
53. Wang, Y.; Zhou, H.; Wu, B.; Zhou, Q.; Cui, D.; Wang, L. Protein Kinase C Isoforms Distinctly Regulate Propofol-induced Endothelium-dependent and Endothelium-independent Vasodilation. *J. Cardiovasc. Pharmacol.* **2015**, *66*, 276–284. [[CrossRef](#)] [[PubMed](#)]
54. Davis, M.D.; Sheetz, M.J.; Aiello, L.P.; Milton, R.C.; Danis, R.P.; Zhi, X.; Girach, A.; Jimenez, M.C.; Vignati, L.; Group, P.-D.S. Effect of ruboxistaurin on the visual acuity decline associated with long-standing diabetic macular edema. *Invest. Ophthalmol. Vis. Sci.* **2009**, *50*, 1–4. [[CrossRef](#)]
55. Aiello, L.P.; Vignati, L.; Sheetz, M.J.; Zhi, X.; Girach, A.; Davis, M.D.; Wolka, A.M.; Shahri, N.; Milton, R.C.; Pkc, D.R.S.; et al. Oral protein kinase c beta inhibition using ruboxistaurin: Efficacy, safety, and causes of vision loss among 813 patients (1,392 eyes) with diabetic retinopathy in the Protein Kinase C beta Inhibitor-Diabetic Retinopathy Study and the Protein Kinase C beta Inhibitor-Diabetic Retinopathy Study 2. *Retina* **2011**, *31*, 2084–2094. [[CrossRef](#)]
56. Joy, S.V.; Scates, A.C.; Bearely, S.; Dar, M.; Taulien, C.A.; Goebel, J.A.; Cooney, M.J. Ruboxistaurin, a protein kinase C beta inhibitor, as an emerging treatment for diabetes microvascular complications. *Ann. Pharmacother.* **2005**, *39*, 1693–1699. [[CrossRef](#)]
57. Chang, F.; Flavahan, S.; Flavahan, N.A. Potential pitfalls in analyzing structural uncoupling of eNOS: Aging is not associated with increased enzyme monomerization. *Am J Physiol Heart Circ Physiol.* **2019**, *316*, H80–H88. [[CrossRef](#)]

**Disclaimer/Publisher’s Note:** The statements, opinions and data contained in all publications are solely those of the individual author(s) and contributor(s) and not of MDPI and/or the editor(s). MDPI and/or the editor(s) disclaim responsibility for any injury to people or property resulting from any ideas, methods, instructions or products referred to in the content.